2015 IEEE International Conference on Advanced Intelligent Mechatronics (AIM)
July 7-11, 2015. Busan, Korea

Experimental Verification of Physical Relation between a Gimbal System and a Body System: GYROBO

S. D. Lee and S. Jung, *Member, IEEE*

***Abstract*—CMGs(Control Moment Gyros) provide an access to control the body's attitude with gimbal's minimum effort. This merit comes from the fact that CMG is based on the gyroscopic effect induced by the motion of a gimbal system with a constantly spinning flywheel. CMG has been used in GYROBO, a single-wheel mobile robot developed at Chungnam National University. The rate of the gimbal motion combined with the angular momentum generated by the rotating flywheel produces the gyroscopic effect onto the body. In the opposite way, the body motion induced by the external disturbances affects the gimbal's motion as well. In this paper, we conduct the experimental verification of the angular rate deviations of the gimbal system interrupted by the disturbance to find the relationship between the body and the gimbal system. Experimental data are justified through the equation approximated by the least square method. Then the experimental results are compared with the derived equation.**

***Index Terms*—CMG, Gimbal angular rate, least square method, gyro effect, GYROBO**

I. Introduction

CMG(Control Moment Gyro) has been studied for a long time after it was firstly implemented in the satellite "Skylab" and the payload "ATM" in 1960s [1]. CMG gives us an access to control the attitude of the body with a gimbal system [2-4].

The concept of CMG has been utilized in the robotics area such as mobile robots, underwater robots, and aerial robots. Typically, GYROBO, a single-wheel mobile robot system developed at Chungnam National University uses the gyroscopic effect to balance itself, and the balancing and driving control tasks were successfully demonstrated [5, 6]. As we apply gyroscopic effect to the dynamical systems, the relationship between the system body and the gimbal system becomes important in designing a new gyroscopic system.

The external disturbance increases the risk of encountering singularities and it must be considered in the design of the control law for CMG [7]. In a CMG, the external disturbance generates a variance in gimbal's motion. This phenomenon is caused by the inverse of the gyroscopic effect. In order to achieve the successful design of the controller, the gimbal motion reacting against the body motion must be explored.

Recently, CMG with a magnetic bearing is an active research topic that both control and energy-saving can be done simultaneously. For the efficient harvest of the energy, the effect of the disturbance must be considered as well [8-11].

When the angular momentum is combined with the motion of the gimbal, the gyroscopic torque is induced onto the system body. However, when the angular moment is combined with the motion of the body, the gyroscopic torque value varies with respect to the angle of a gimbal. The misaligned flywheel causes both the attitude control problem and the energy loss problem. In case of multi-axis CMGs, this problem becomes more severe due to the complexity in estimating the motion of the gimbal.

The study on the rejection of the gyroscopic effect of CMG also has been studied. In [7], the simple way for the gimbal angle compensation is introduced. They used the magnetic control law to solve the problem [8-10] in which the system was a magnetically suspended CMG. They introduced the clean control method to compensate the magnetic bearing's vibration induced by gyroscopic effects.

In the previous research, it is found that the gimbal loses the control ability when it leans over the threshold angle from its original attitude [6]. One of the control problems about the CMG is the limitation of the available tilt angle. The controller should impose a restriction on the gimbal motion in some manner. Experiences lead us to investigate the relationship between the rate of a gimbal and the rate of a system body further.

Therefore, in this paper, the physical relation between a gimbal system and a system body is investigated in detail. Firstly, we investigate the motion variance of the gimbal from the angular momentum of the flywheel. Secondly, the experimental studies are conducted to confirm the equation by gathering data. During this procedure, the least square fitting method is used. Finally, the difference between the value by the equation and by the experimental studies is analyzed. This idea will help us to design a new CMG, control it, and monitor

This work was supported in part by the 2013 General research program of Korea Research Foundation (KRF) and the 2014 the basic research funds through the contract of National Research Foundation of Korea (NRF-2014R1A21A11049503).

S. D. Lee and S. Jung are with Department of Mechatronics Engineering, Chungnam National University, Daejeon, Korea 305-764
(e-mail: jungs@cnu.ac.kr)

the state of CMG in a very intuitive way.

II. Principle of Gyroscopic Motion

A. Yawing motion

The main goal of GYROBO is to maintain balance by yawing motion induced by the gyroscopic effect which is described in Fig. 1. A flywheel rotates about x_1 axis at a constant speed to generate the angular momentum vector $\mathbf{A}$. When the roll motion is controlled by the y_1' axis, the motion about the z_1 axis is induced as an output. $\boldsymbol{\omega_g}$ is the angular velocity vector of the gimbal, $\boldsymbol{\Omega}$ is the angular velocity vector of the body, and $\Delta\theta$ is the deviation angle between the gimbal and the body according to the motion of the angular momentum vector $\mathbf{A}$.

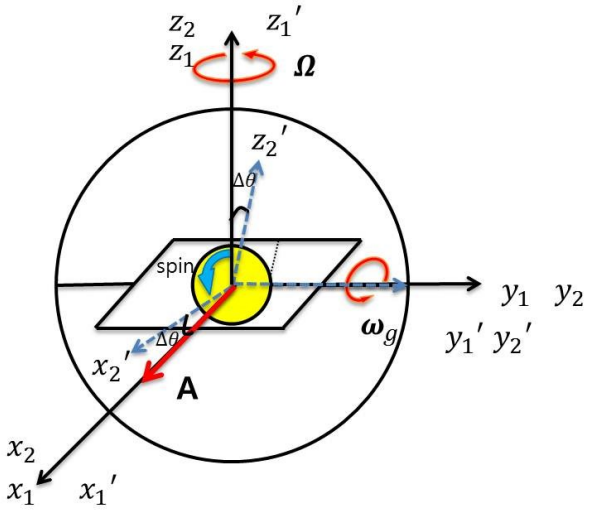

Fig. 1 Coordinate of the yawing motion

The coordinate axis (x_1, y_1, z_1) is the reference of the body, (x_2, y_2, z_2) is the moving coordinate axis of the body, (x_1', y_1', z_1') is the reference of the gimbal, (x_2', y_2', z_2') is the moving coordinate of the gimbal.

For a rigid body, the rate difference of the coordinate axis of the system can be described as follows.

$$\frac{d\mathbf{A}}{dt} - \frac{d\mathbf{A}'}{dt} = \boldsymbol{\Omega} \times \mathbf{A} \tag{1}$$

where the magnitude of vector $\boldsymbol{\Omega}$ is Ω and the magnitude of vector $\mathbf{A}$ is L. The time differential of $\mathbf{A}$ is the variance of the vector $\mathbf{A}$ along the (x_1, y_1, z_1) coordinate axis. And the time differential $\mathbf{A'}$ is the variance of the vector $\mathbf{A'}$ along the (x_1', y_1', z_1') coordinate. During the body motion, the time differential of $\mathbf{A}$ is zero because x_1 is equal to x_2. But, the time differential of $\mathbf{A'}$ is same as $\boldsymbol{\omega_g}$.

The magnitude of (1) becomes

$$0 - \omega_g = \Omega L \sin(\pi/2 + \Delta\theta) \tag{2}$$

where ω_g is the magnitude of vector $\boldsymbol{\omega_g}$.

Initially, $\Delta\theta = 0$, (2) becomes

$$\omega_g = -\Omega L \tag{3}$$

In (3), we derive the rate equation when the body axis is orthogonal to the gimbal axis. The magnitude of the gimbal rate is proportional to the body rate multiplied with the angular momentum of the flywheel. The rate of the gimbal is inferred with this equation.

B. Rolling motion

In the rolling motion, the velocity of the body axis coordination is the same as the velocity of the gimbal axis coordination as shown in Fig. 2. Assume the initial deviation angle as $\Delta\theta_1$ and the next deviation angle as $\Delta\theta_2$. In this configuration, these values are always zero. According to this, the equation of this configuration is shown as follows.

$$\Omega - \omega_g = \omega_g L \sin(\Delta\theta) = 0 \tag{4}$$

since $\Delta\theta = \Delta\theta_1 = \Delta\theta_2 = 0$. Then (4) becomes

$$\omega_g = \Omega \tag{5}$$

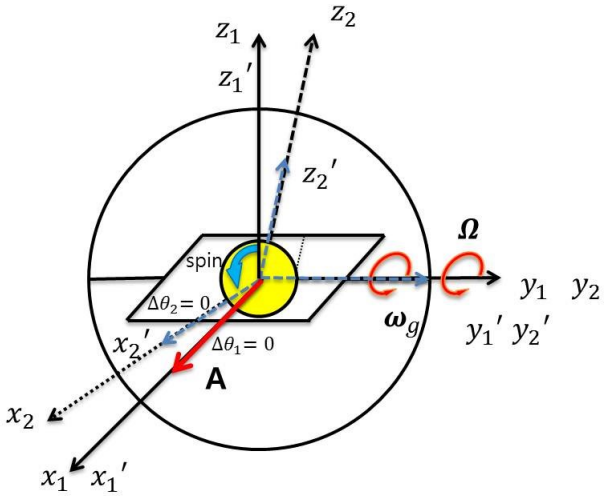

Fig. 2 Coordinate of the rolling motion

In a control design viewpoint, the gimbal's attitude initially keeps standing upright its attitude. When the external disturbance affects the body, the function of the gimbal is lost. Therefore, the derivation of the relationship between the two rate equations is important to understand the system better. Based on this concept, the attitude of the body can be controlled by overcoming the limitation of the gimbal.

Since the angular momentum of the flywheel in a CMG has a constant value, the disturbance rate is proportional to the value of the angular momentum. From this, the control law can be easily designed to change the direction of the gimbal under the presence of disturbance.

III. GYROBO SYSTEM

The GYROBO system is composed of three parts: a gimbal system with a flywheel, a body wheel, and control hardware. A gimbal system consists of a flywheel, a flywheel motor, a tilting motor and a housing part.

A. Flywheel

The configuration of a flywheel is shown in Fig.3. The inertia of a disc about the central axis is calculated as

$$I_r = \frac{1}{2}mr^2 \tag{6}$$

where m is the mass and r is the radius of the flywheel.

In our system, system parameters are given as m is 2.1 kg, r is 0.075 m, and δ is 0.016 m. Then the moment of inertia can be obtained as

$$I_r = \frac{1}{2}mr^2 = \frac{1}{2}\times 2.1\times 0.075^2 = 0.005906(kgm^2) \tag{7}$$

Then the angular momentum is calculated by

$$L = I_r\omega = 0.005905\omega(Nms) \tag{8}$$

where ω is the angular velocity of the flywheel.

TABLE I
PARAMETERS' DESCRIPTION OF THE GIMBAL SYSTEM

Symbol	Definition	Units
m	Mass of the flywheel	kg
r	Radius of the flywheel	$meter$
δ	Width of the flywheel	$meter$
I	Moment of inertia of the flywheel	kgm^2
ω	Angular velocity	rad/s
L	Angular momentum	$kgm^2 rad/s$

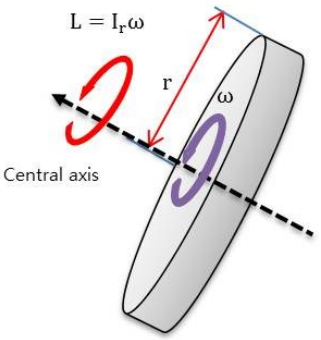

Fig. 3 Flywheel configuration

B. Motor, Driver, and Control

A 198 watt-level DC motor is used to rotate the flywheel. A motor driver has an ability to drive +12VDC/50A continuous source to the motor. The motor driver is controlled by the PWM(Pulse Width Modulation) signal generated from the control hardware.

The motor specification is shown in Fig. 4.

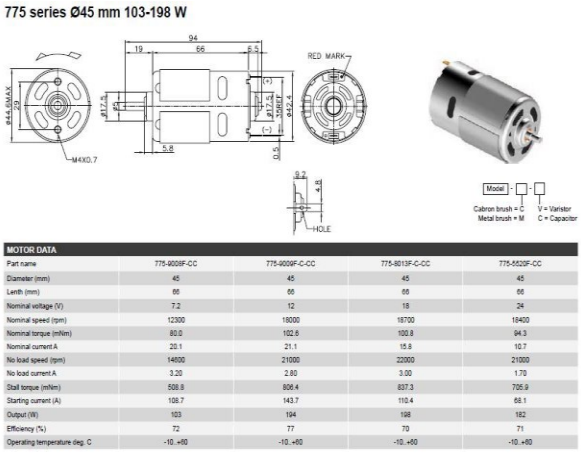

MOTOR DATA				
Part name	775-9008F-CC	775-9009F-C-CC	775-8013F-C-CC	775-5520F-CC
Diameter (mm)	45	45	45	45
Lenth (mm)	66	66	66	66
Nominal voltage (V)	7.2	12	18	24
Nominal speed (rpm)	12300	18000	18700	18400
Nominal torque (mNm)	80.0	102.6	100.8	94.3
Nominal current A	20.1	21.1	15.8	10.7
No load speed (rpm)	14600	21000	22000	21000
No load current A	3.20	2.80	3.00	1.70
Stall torque (mNm)	508.8	806.4	837.3	705.9
Starting current (A)	108.7	143.7	110.4	68.1
Output (W)	103	194	198	182
Efficiency (%)	72	77	70	71
Operating temperature deg. C	-10..+60	-10..+60	-10..+60	-10..+60

Fig. 4 Motor specification

The driver is shown in Fig. 5. The full power of the driver is about 600 Watts and the power of the motor for the flywheel is about 200 Watts. The driver was selected to control two motors instantaneously. The output current is controlled by the PWM voltage of the controller. The driver contains the MOSFET(Metal Oxide Silicon Field Effect) elements as a gate to drive the current to the motor. MOSFET has the voltage-controlled-current-output characteristic. This ability of microelectronics can lead us to control the current of the driver easily using the voltage control signal like PWM.

From the driver, we can calculate the current range of the control. Considering the motor power, the maximum current value is 16 amperes which is 32 percent of the full PWM control range. Therefore, the current level is divided into 16 steps to have the maximum of 16 amperes as listed in Table II.

Item	Range
Input Voltage Range	15V ~ 50V
Continuous Current	50A
Output Voltage	+12V
Control Method	PWM (0~999)

Fig. 5 Driver specification

We use a DSP as a controller of the system which sends the PWM command periodically through a serial communication port. The command protocol includes the velocity information which must be fulfilled by the motor driver. The relationship among commands, currents and speeds is listed in Table II.

Fig. 6 shows the typical control command STEP 14 as an example. The duty ratio of PWM is 28 percent and the driving current is 14A. The expected RPM(Revolution Per Minute) of the motor is about 5,000. The flywheel in a gimbal is mounted

to the motor and the motor is rotated by the programmed command like this. The allowable command is limited by STEP 16 where the flywheel rotates about 5,700 RPM.

TABLE II
Control command characteristics

step	controller command	driver duty(%)	motor	
			current(A)	speed(RPM)
1	020	2	1	
2	040	4	2	
3	060	6	3	
4	080	8	4	
5	100	10	5	
6	120	12	6	2200
7	140	14	7	2550
8	160	16	8	2900
9	180	18	9	3250
10	200	20	10	3600
11	220	22	11	3950
12	240	24	12	4300
13	260	26	13	4650
14	280	28	14	5000
15	300	30	15	5350
16	320	32	16	5700

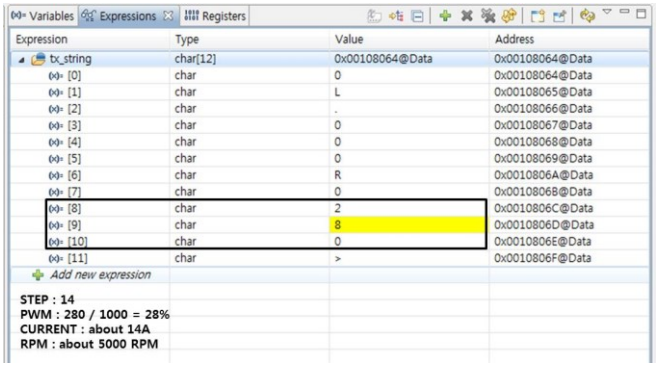

Fig. 6 STEP 14 command data

C. *Overall system structure*

Yawing and rolling are the motions of the body and rotating and tilting are the motions of the flywheel. The flywheel has an angular momentum L when the flywheel spins as an angular velocity ω. The added motion of the rate of the tilting to the angular momentum generates a torque to the body. As a result, the body's orientation can be controlled by the gimbal's motion.

The conceptual model of the system is described in Fig. 7, which shows the relationship between a gimbal and a body when two different components are combined with the flywheel.

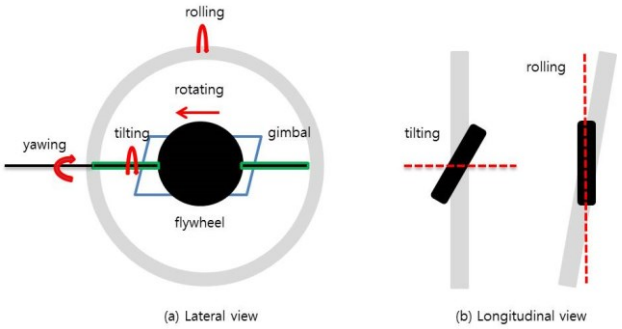

Fig. 7 Overall system structure

In a body control problem, a gimbal is the control input and a body becomes a control output of the system as a forward manner. In this mode, the gimbal's attitude must be kept in a limited angle. In the inverse manner, a gimbal is the output and a body motion becomes a control input as shown in Fig. 8.

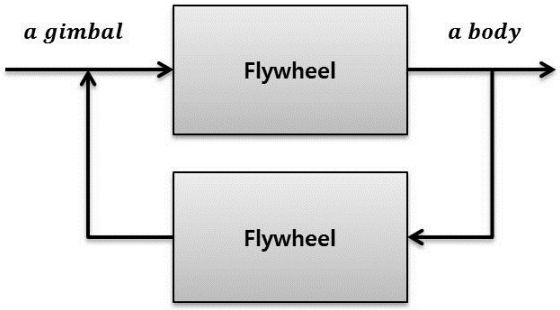

Fig. 8 Forward and inverse manners

IV. EXPERIMENTAL STUDIES

A. *Experimental setup*

The disturbance effects onto the gimbal in CMG are demonstrated in Fig. 9 by tilting the body. Fig. 9 (a) represents that the rolling motion of the body has no effect onto the gimbal's attitude deviations. When we shake the body by hands in the rolling direction, no variance of the attitude of the gimbal is observed. Fig. 9 (b) shows that the yawing variance of the body generates the tilting variance of the gimbal's attitude.

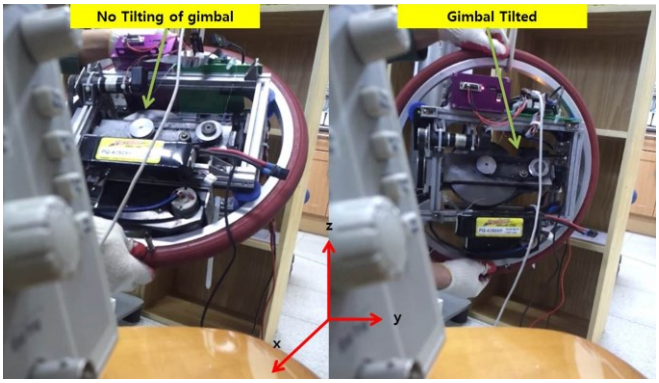

(a) Rolling motion (b) yawing motion
Fig. 9 Backward gyroscopic effect

As the speed of the body motion goes up, the rate of the gimbal's attitude variance also is increased. Shaking the body by hands is considered as the disturbance from the external sources. The external disturbance induces the variance of the gimbal's attitude.

The overall experimental setup is shown by Fig. 10.

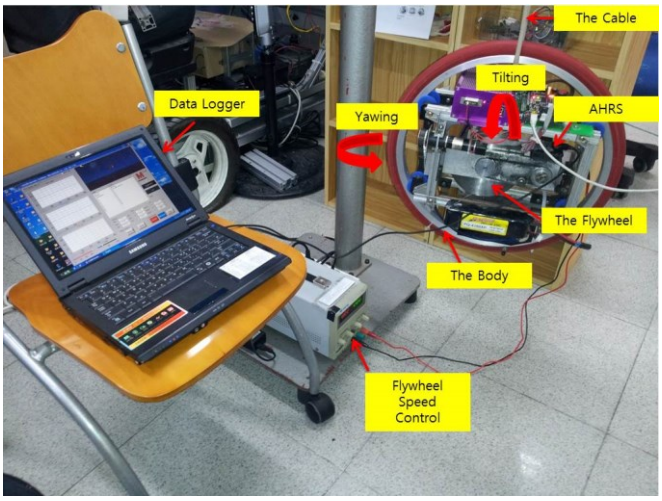

Fig. 10 Experimental setup

AHRS sensor is the attitude and heading reference system that contains 3-axis gyro, 3-axis-accel, and 3-axis-magnet. The problems of gyro's drift and the low bandwidth of an accelerometer are reduced by the filter algorithm shown in Fig. 11.

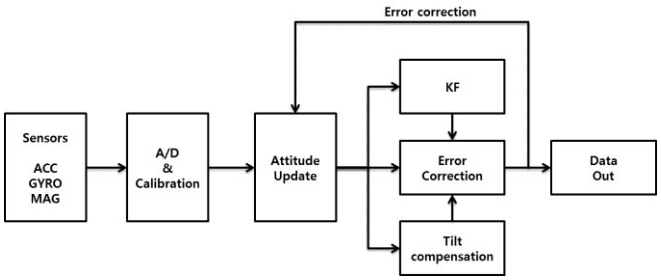

Fig. 11 AHRS algorithm [12]

B. Experimental results

Data logger collects the attitude, the rate, and the acceleration data from the AHRS sensor with 100 Hz bandwidth. During the experiment, the speed of the flywheel in a gimbal is controlled. The digital power supply instead of the battery of the system is used.

We shake and lean the body to collect the reaction data from the sensor. The collected data plots are shown in Fig. 12. Data are collected when steps 5, 6, 7, 9, 13 and 15 are used.

As the speed of the flywheel increases, the relationship between the body and the gimbal is strongly coupled. The x-axis is the body disturbance and the y-axis is the gimbal motion in Fig. 12. When we shake the body repeatedly by using hands, this makes the data feature like a cloud.

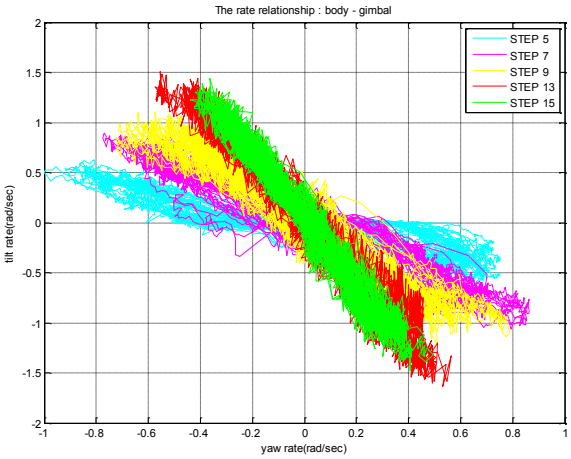

Fig. 12 Body-gimbal relationship

As shown in Fig. 12, the gimbal attitude deviation is occurred by the body's motion. This stems from the unwanted gyroscopic effect in this paper. When the gimbal loses its orientation affected by the disturbance of the body, the function of the gimbal is lost because the gimbal is basically mounted to the body to generate the gyroscopic effect onto the body not to be affected by the body.

C. Data analysis

Lines to represent the cloudy data using a least square method are found. The least square method is a procedure to determine the best line to fit the data. The purpose of the least square method is to find the coefficients of the equation (10).

$$y = b + ax \tag{10}$$

Fig. 13 shows that the result out of the least square linearization. Five sorts of cloudy data are represented by the straight lines and the respective coefficients are plotted. The value b is nearby the zero value.

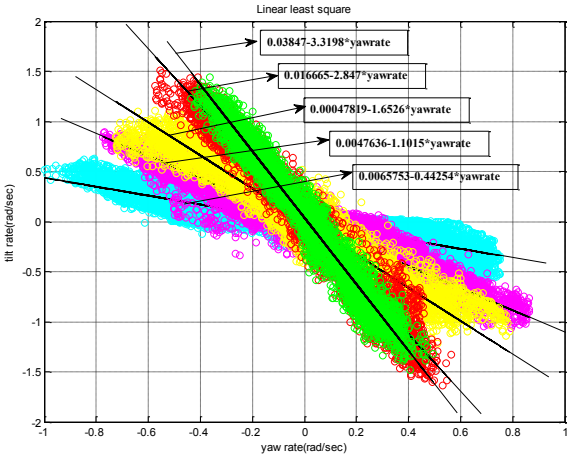

Fig. 13 Least square fitting result

After fitting, we investigate the coefficient and compare it with the expected value calculated by hand in advance. The slopes of the curve actually represent the value of the angular momentum of the flywheel.

Table III lists the values used in the experimental studies. Note that the angular momentum L found by the hand calculation and by experimental results when two different step commands step 13 and step 15 are applied. The number of data collected for step 13 is 4084. The average is 0.0083(rad/sec) and the variance is 0.2538(rad/sec). The number of data collected for step 15 is 4491 and the average is 0.01(rad/sec) and the variance is 0.2045(rad/sec).

The difference between the calculation and the experiment is less than 0.01 for step 15 and 0.03 for step 13, which is quite close to each other. This confirms that our analysis through experimental studies to find the angular momentum values is quite correct.

TABLE III
COMPARISON BETWEEN EXPERIMENT AND THEORIES

STEP	15	13
m(kg)	2.1	2.1
r(m)	0.075	0.075
I=1/2MR^2(kgm^2)	0.00590625	0.00590625
rpm	5350	4650
w(rad/s)	560.2506899	486.9468613
L(By hand)	3.308980637	2.8760299
L(Experiment)	3.3198	2.847
Difference	-0.010819363	0.0290299

V. CONCLUSION

The equation of the rate relationship between the gimbal and the body was derived. The relational data between the gimbal and the body were collected by the extensive experimental studies. Experimental data have been analyzed by the least square method to find the line equation to fit the data. The resulting difference is less than 0.01 kilogram-square meter radian per second in the step 15 which means that the theoretical and experimental values are quite close to each other. This approach will reduce the time to design and control the CMG in considering the effect of the external disturbance.

REFERENCES

[1] L. Morine L., et al. *Control Moment Gyroscope Gimbal Actuator Study*. BENDIX CORP TETERBORO NJ ECLIPSE-PIONEER DIV, 1966.

[2] Nazareth S. Bedrossian, et al. "Steering law design for redundant single-gimbal control moment gyroscopes." *Journal of Guidance, Control, and Dynamics* 13.6 (1990): 1083-1089.

[3] Y. Nakamura and H. Hideo, "Inverse kinematic solutions with singularity robustness for robot manipulator control." *Journal of dynamic systems, measurement, and control* 108.3 (1986): 163-171.

[4] S. R. Vadali, "Feedback control and steering laws for spacecraft using single gimbal control moment gyros." *J. Astronaut. Sci* 39.2 (1991): 183-203.

[5] P. K. Kim, J. H. Park, and S. Jung. "Experimental studies of balancing control for a disc-typed mobile robot using a neural controller: GYROBO." *Intelligent Control (ISIC), 2010 IEEE International Symposium on*. IEEE, 2010.

[6] J. H. Park and S. Jung. "Development and control of a single-wheel robot: Practical Mechatronics approach." *Mechatronics* 23.6 (2013): 594-606.

[7] V. J. Lappas, W. H. Steyn, and C. I. Underwood. "Control moment gyro (CMG) gimbal angle compensation using magnetic control during external disturbances." *Electronics Letters* 37.9 (2001): 603-604.

[8] J. C. Fang and Y. Ren, "Decoupling control of magnetically suspended rotor system in control moment gyros based on an inverse system method." *Mechatronics, IEEE/ASME Transactions on* 17.6 (2012): 1133-1144.

[9] Y. Ren and J. C. Fang. "High-stability and fast-response twisting motion control for the magnetically suspended rotor system in a control moment gyro." *Mechatronics, IEEE/ASME Transactions on* 18.5 (2013): 1625-1634.

[10] J. C. Fang and Y. Ren. "High-precision control for a single-gimbal magnetically suspended control moment gyro based on inverse system method." *Industrial Electronics, IEEE Transactions on* 58.9 (2011): 4331-4342.

[11] Z. S. Wang. "Application of Adaptive Interference Suppressor to Gimbal of MSCMG." *Digital Manufacturing and Automation (ICDMA), 2013 Fourth International Conference on*. IEEE, 2013.

[12] Microinfinity: http://www.minfinity.com